Challenges in coupled-channels calculations of heavy-ion fusion reactions

Henning Esbensen

Argonne National Laboratory, Argonne IL 60439, USA

The approximations that are commonly made in coupled-channels calculations of heavy-ion fusion reactions are reviewed in order to show where uncertainties exist and improvements can be made. In particular, the failure in modeling the fusion at extreme subbarrier energies is discussed.

§1. Introduction

Heavy-ion fusion is a sensitive probe of the structure and the size of the reacting nuclei.[1] This is most clearly seen in coupled-channels analyses of the fusion cross sections measured on a series of isotopes with the same projectile. There are several uncertainties in such analyses that I would like to point out, namely, in the nuclear interaction between the ions, in the structure input, and in the truncation of the coupled channels considered. The calculations are usually performed in the so-called rotating frame approximation, and the couplings that excite the reacting nuclei are usually derived in a macroscopic model. The fusion process by itself is simulated by in-going-wave boundary conditions, which are imposed somewhere inside the Coulomb barrier.

When analyzing fusion data one should be aware of all of these uncertainties and approximations. This is particularly important when analyzing high precision fusion data. In order to generate a good fit to the data, one may be tempted to use interactions or form factors that are unrealistic and inconsistent with scattering data. One way to avoid this danger is to analyze elastic and inelastic scattering data within the same coupled-channels calculation that is used to calculate the fusion. Such calculations may be difficult and time-consuming because it is necessary to include all the reaction channels that have an effect on fusion, and also all the channels that can affect the scattering observables of interest. Another problem is that the rotating frame is not reliable at smaller scattering angles, so one would have to go beyond this approximation and include full angular momentum coupling. This would make the calculation even more challenging.

While the elastic and inelastic scattering is sensitive mostly to the interaction and form factors at large radial separations,[2] say outside the Coulomb barrier, the fusion is primarily sensitive to the these quantities in the vicinity of the Coulomb barrier.[3] Recently it has been recognized that coupled-channels calculations of fusion can also be sensitive to the interactions inside the Coulomb barrier. This has become evident from calculations performed at extreme subbarrier energies.[4]

I will illustrate some of the features of coupled-channels calculations by presenting results for the fusion of ^{27}Al+^{74}Ge. I will also discuss the behavior of fusion

typeset using $\mathcal{PTP}$TEX.cls ⟨Ver.0.89⟩

cross sections at extreme subbarrier energies, where an unexpected steep falloff with decreasing energy has been observed for several heavy-ion systems.[5)]

§2. Macroscopic description of surface modes

In the macroscopic model of heavy-ion reactions,[6)] the surface of a nucleus is parametrized as

$$R_i(\hat{r}, \alpha_{\lambda,\mu}) = R_i\Big(1 + \sum_{\lambda\mu} \alpha^{(i)}_{\lambda\mu}\ Y^*_{\lambda\mu}(\hat{r})\Big), \tag{2·1}$$

where $\hat{r}$ specifies a spatial direction and $\alpha^{(i)}_{\lambda\mu}$ are the so-called deformation amplitudes. The latter amplitudes generate rotational excitations or vibrational excitations of surface modes. One assumes furthermore that the nuclear interaction is a function $V_N(\Delta s)$ of the surface-surface distance Δs between the reacting nuclei,

$$\Delta s = r - R_1 - R_2 - \delta R, \tag{2·2}$$

where

$$\delta R = \sum_{\lambda\mu} R_1 \alpha^{(1)}_{\lambda\mu} Y^*_{\lambda\mu}(\hat{r}) + R_2 \alpha^{(2)}_{\lambda\mu} Y^*_{\lambda\mu}(-\hat{r}) \tag{2·3}$$

is measured along the spatial separation $\mathbf{r}$ of the two nuclei.

2.1. *Interactions*

The ion-ion potential is defined as the ground state expectation of the nuclear interaction,

$$U(r) = \langle \text{g.s.}|\ V_N(r - R_1 - R_2 - \delta R)\ |\text{g.s.}\rangle. \tag{2·4}$$

To calculate matrix elements of the interaction $V_N(\Delta s)$ one would need a structure model for the excited states of the two nuclei. The simplest approach is to consider rotational excitations or pure harmonic vibrations. A more general description in terms of anharmonic vibrations was recently applied.[7)]

A great advantage of the harmonic oscillator model for vibrational excitations is that the matrix elements of V_N can be expressed in terms of derivatives of the ion-ion potential $U(r)$ (a general expression is given in appendix A of Ref. 8). Thus we do not need to know V_N but can instead use $U(r)$ and parametrize it, for example, as a Woods-Saxon well. If we only consider excitations of one- and two-phonon states, then all the necessary matrix elements can be generated (to leading order in the deformation amplitudes) from the following linear and quadratic interactions

$$\delta V^{(1)}_N = -\frac{dU(r)}{dr}\ \delta R, \tag{2·5}$$

$$\delta V^{(2)}_N = \frac{1}{2}\frac{d^2U(r)}{dr^2}\ \Big[(\delta R)^2 - \langle \text{g.s.}|\ (\delta R)^2\ |\text{g.s.}\rangle\Big]. \tag{2·6}$$

Another approach is to start with a parameterization of the interaction V_N and then calculate the matrix elements explicitly.[9),10)] One problem is that the ion-ion potential, Eq. (2·4), and also other form factors, would become more and more

diffuse as one included more and more states.[9] It is therefore much more appealing to start from an empirical parameterization of the ion-ion potential $U(r)$.

Matrix elements of the Coulomb interaction can be generated from the linear interaction

$$\delta V_C^{(1)} = \sum_{\lambda\mu} \frac{3Z_1 Z_2 e^2}{(2\lambda+1)r^{\lambda+1}} \Big[R_{C1}^{\lambda}\ \alpha_{\lambda\mu}^{(1)}\ Y_{\lambda\mu}^*(\hat{r}) + R_{C2}^{\lambda}\ \alpha_{\lambda\mu}^{(2)}\ Y_{\lambda\mu}^*(-\hat{r}) \Big], \qquad (2{\cdot}7)$$

whereas the quadratic and higher-order Coulomb fields are less important,[10] and they are therefore often ignored.

2.2. *Structure model dependence*

There are basically two ways one can determine the matrix elements of the interactions Eqs. (2·5-2·7). One way is to adopt a particular structure model, such as a harmonic oscillator, a rotational model, or an anharmonic vibration.[7] The advantage of these models is that one can calculate all the matrix elements that are needed. The other approach is to determine the matrix elements from other measurements, such as inelastic scattering. Here the disadvantage is that many of the matrix elements are not known; the most one can hope for is matrix elements of the linear interactions Eqs. (2·5,2·7).

The deformation amplitudes that appear in the Coulomb and nuclear fields, respectively, are in principle different. However, matrix elements of the nuclear amplitudes are often unknown, so to proceed one assumes that they are identical to the corresponding electromagnetic matrix elements. In either case, the direct matrix element of the deformation amplitude, between the ground state and an excited state, is expressed in terms of the β-value,

$$\langle \lambda\mu | \alpha_{\lambda\mu} | \text{g.s.} \rangle = \frac{\beta_\lambda}{\sqrt{2\lambda+1}}. \qquad (2{\cdot}8)$$

This expression is independent of the particular nature of the excited state (vibrational or rotational). Diagonal matrix elements of the linear interaction, on the other hand, are model dependent. They always vanish in the vibrational model but they can be non-zero in the rotational limit. An example is the 2^+ state in a quadrupole deformed nucleus. Here one has the diagonal matrix element

$$\langle 20 | \alpha_{20} | 20 \rangle = -\sqrt{\frac{5}{16\pi}}\ \frac{4\pi Q_2}{3ZeR_C^2}, \qquad (2{\cdot}9)$$

which is expressed in terms of the quadrupole moment Q_2 of the 2^+ state.

The diagonal matrix elements of the quadratic interaction $\delta V_N^{(2)}$ are also model dependent. Thus for a vibrational one-phonon state $|\lambda\mu\rangle$ one finds that

$$\langle \lambda\mu | \delta V_N^{(2)} | \lambda\mu \rangle = \frac{d^2U}{dr^2}\ \frac{(\beta_\lambda R)^2}{4\pi}, \qquad (2{\cdot}10)$$

whereas in the rotational limit one obtains

$$\langle 20 | \delta V_N^{(2)} | 20 \rangle = \frac{4}{7}\ \frac{d^2U}{dr^2}\ \frac{(\beta_2 R)^2}{4\pi} \qquad (2{\cdot}11)$$

for the $|2^+, m = 0\rangle$ state. The off-diagonal matrix elements of the quadratic interaction are less model dependent because they can be expressed as products of linear matrix elements (see appendix A of Ref. 8). This is very fortunate because the off-diagonal matrix elements have a much larger influence on subbarrier fusion than the diagonal have.[20)]

2.3. *The ion-ion potential*

An important issue is how to determine the ion-ion potential. In most coupled-channels calculations of fusion one uses a real and energy-independent ion-ion potential, and one tries to include explicitly the couplings to all channels that can affect the fusion. When analyzing scattering data, on the other hand, one employs energy dependent complex optical potentials. The imaginary part is introduced to simulate the effect of absorption into channels that are not included explicitly.

It has been recognized that the real and the imaginary parts of the empirical optical potentials for elastic scattering are (approximately) related by a dispersion relation.[11)] The rather sudden disappearance of the 'absorption' at energies below the Coulomb barrier implies (via the dispersion relation) a strong energy dependence of the real part of the optical potential at energies near the Coulomb barrier. This is referred to as the threshold anomaly.[11)]

In coupled-channels calculations, where one uses an energy-independent ion-ion potential, one generates effectively an energy dependent polarization potential, for example, in the elastic scattering channel. The real and imaginary parts of the polarization potential are also related by a dispersion relation.[12)] It is therefore clear that the ion-ion potential one should use is not unique but depends on the states that are included explicitly (or rather not included) in the calculations. A good example of this dependence is illustrated in Ref. 13). Here the effect of the 3^- state in ^{16}O, which has a rather high excitation energy of 6.13 MeV, is shown to produce an adiabatic potential renormalization. Couplings to this state lead to a constant shift in energy of the calculated fusion cross section, but the shape of the cross section as a function of energy is essentially unaffected.

An empirical potential has been extracted from elastic scattering data.[2)] The analysis was based on the observation that the real part of the ion-ion potential is best determined for classical trajectories that lead to rainbow scattering. The extracted potential has been parametrized as a proximity type potential of the form[6)]

$$U(r) = -\frac{R_1 R_2}{R_1 + R_2} \, \frac{16\pi\gamma a}{1 + \exp[(r - R_1 - R_2)/a]}. \tag{2·12}$$

The parameters of this interaction are given in section III of Ref. 6). Roughly speaking, the diffuseness is of the order $a \approx 0.63$ fm, and the nuclear radii are $R_i \approx 1.2\ A^{1/3}$. The maximum nuclear force is consistent with the proximity force between two touching spheres (with a nuclear surface tension of $\gamma \approx 1$ MeV/fm^2). This interaction is a good starting point for coupled-channels calculations; often only minor adjustments are needed to achieve a reasonable fit to data. It is also reassuring to know that the exponential tail of the interaction is in good agreement with folding model predictions (see section III of Ref. 6).

§3. Rotating frame approximation

Coupled-channels calculations of fusion are usually performed in the so-called iso-centrifugal approximations,[14] where one assumes that the orbital angular momentum L for the relative motion of projectile and target motion is conserved. This approximation allows one to choose the z-axis along the center of mass distance $\mathbf{r}$, and it is therefore also referred to as the rotating frame approximation.[15),16] This approximation implies that the magnetic quantum number M of the initial intrinsic spin of the reacting nuclei is also a conserved quantity, because the $\mu = 0$ component is the only component of the interactions that survives when $\hat{r} = \hat{z}$, c.f. Eq. (2·3).

Let us by $|nM\rangle$ denote the states of interest in a coupled-channels calculation, as for example the single and double excitations, and also the mutual excitations, of the low-lying 2^+ and 3^- states in projectile and target. The total wave function has the following form in the rotating frame approximation

$$\Psi_M = \frac{i}{2k_0 r} \sum_{n,L} \phi_n^{LM}(r)\ |nM\rangle\ P_L(\cos(\theta)), \tag{3·1}$$

where M denotes the conserved projection of the intrinsic spin on the rotating z-axis, and $\hbar k_0$ is the relative momentum in the entrance channel. The main reason for making the rotating frame approximation is that the number of coupled channels is considerably smaller than when the angular momentum coupling is treated correctly. A state with spin λ^π, for example, is represented by only one channel in the rotating frame approximation, whereas at least $\lambda + 1$ channels will be needed in general.

3.1. *Coupled equations*

For each (L, M) one has now the following set of coupled differential equations for the radial wave functions,

$$\Big[H_0 + E_n - E\Big]\phi_n^{LM}(r) = -\sum_{n'} \langle nM|\delta V|n'M\rangle\ \phi_{n'}^{LM}(r), \tag{3·2}$$

where

$$H_0 = \frac{\hbar^2}{2M_0}\Big(-\frac{d^2}{dr^2} + \frac{L(L+1)}{r^2}\Big) + \frac{Z_1 Z_2 e^2}{r} + U(r) \tag{3·3}$$

is the Hamiltonian for radial wave function in the elastic channel when all couplings on the r.h.s. of Eq. (3·2) are set equal to zero. The r.h.s. of Eq. (3·2) contains the diagonal and off-diagonal matrix elements of the interaction $\delta V = \delta V_C^{(1)} + \delta V_N^{(1)} + \delta V_N^{(2)} + ...$, consisting of the linear and quadratic interactions, Eqs. (2·5-2·7), and possibly higher-order interactions if needed.

The coupled equations (3·2) are solved with the usual scattering boundary conditions at large distances

$$\phi_n^{LM}(r) \to \delta_{n,0} \exp(-ik_0 r) + R_n^{LM} \exp(ik_n r),\ \text{for } r \to \infty, \tag{3·4}$$

where $\hbar k_n$ are the asymptotic momenta. In-going-wave boundary conditions are imposed inside the barrier,

$$\phi_n^{LM}(r) \to T_n^{LM} \exp(-i\kappa_n r),\ \text{for } r = R_F, \tag{3·5}$$

where $\hbar\kappa_n$ are the local channel-dependent momenta at $r = R_F$. The conditions (3·5) are imposed, for example, at the radial separation where the Coulomb plus nuclear potential has a local minimum.

The fusion cross section is determined by the ingoing flux at R_F. One can also simulate the fusion by the absorption from a short-ranged imaginary potential. In either case, one should solve the coupled equations (3·2) for all values of the initial spin projection, $M = -I, ..., I$, where I is the initial intrinsic spin and determine the fusion cross section σ_{fM} in each case. The total fusion cross section is then the average value,

$$\sigma_f = \frac{1}{2I+1} \sum_M \sigma_{fM}. \tag{3·6}$$

§4. Diagnostic tools

There are several tools available when comparing coupled-channels calculations to data. The simplest is the χ^2 value but that does not reveal where the discrepancies occur. A way to emphasize the energy dependence of fusion cross sections near the Coulomb barrier is to calculate the barrier distribution, which is defined as[17)]

$$B(E) = \frac{d^2}{dE^2}(E\sigma_f). \tag{4·1}$$

It ts calculated by the finite difference method with appropriate energy steps (as discussed in Ref. 18). This distribution reflects the effect of couplings to different channels. This connection is most clearly seen in the work of Dasso et al.,[3)] where the fusion cross section is obtained from diagonalizing the interaction Hamiltonian at the Coulomb barrier.

The barrier distribution vanishes at extreme subbarrier energies but here another useful tool is available, namely, the logarithmic derivative[5)]

$$L(E) = \frac{d}{dE} \ln(E\sigma_f) = \frac{1}{E\sigma_f} \frac{d}{dE}(E\sigma_f). \tag{4·2}$$

Finally one can also use the S factor which is defined as

$$S(E) = E\sigma_f \ \exp(2\pi\eta), \ \text{where } \eta = \frac{Z_1 Z_2 e^2}{\hbar v} \tag{4·3}$$

is the Sommerfeld parameter. The S factor is a good representation of light-ion fusion and capture reactions but it is also a useful representation for heavy-ion fusion at extreme subbarrier energies.[4),19)]

From the two definitions, Eqs. (4·2,4·3), one can derive the following expression for the logarithmic derivative when the S factor is assumed to be a constant,

$$L_{CS}(E) = \frac{\pi\eta}{E}. \tag{4·4}$$

This is a useful extreme limit to consider when analyzing the logarithmic derivatives extracted from measurements.

§5. Application to the fusion of ^{27}Al + ^{74}Ge.

I have recently performed coupled-channels calculations[20] of the fusion of ^{27}Al with a series of germanium isotopes and compared the results to measurements.[21] The purpose was to see whether the fusion data can put constraints on the quadrupole moments of the germanium isotopes. It appears that the measurements of the quadrupole moment of the 2^+ state have two solutions,[22] namely, one associated with a near spherical shape and one with a significant prolate deformation. The largest deformation is expected in ^{74}Ge. The analysis of the fusion data showed, however, that the near spherical shape is preferred for ^{74}Ge.

The $5/2^+$ ground state of ^{27}Al has a quadrupole moment of $Q = 15$ e fm^2. This implies that the radial Hamiltonian (3·3) for the elastic scattering channel must be supplemented by the M-dependent quadrupole interaction,

$$\delta V^{(1)}_{2M} = \langle 5/2, M|\alpha_{20}|5/2, M\rangle \sqrt{\frac{5}{4\pi}} \left(-R_N \frac{dU(r)}{dr} + \frac{3Z_1Z_2e^2}{5r^3}R_C^2\right). \tag{5·1}$$

The nuclear part is equivalent (to lowest order) to an M-dependent radius of ^{27}Al,

$$R(M) = R_N\left(1 + \langle 5/2, M|\alpha_{20}|5/2, M\rangle\sqrt{\frac{5}{4\pi}}\right). \tag{5·2}$$

The effect on fusion is shown in Fig. 1. The dashed curves show in increasing order the calculated fusion cross sections for $M = 1/2$, $3/2$, and $5/2$. The solid curve shows the average fusion cross section. It is in good agreement with the data.[21] The reduced χ^2 based on the statistical uncertainty is 5.5, but this value is reduced to 2.8 if one includes an estimated systematic error of 3%. The associated barrier distributions are shown in Fig. 2.

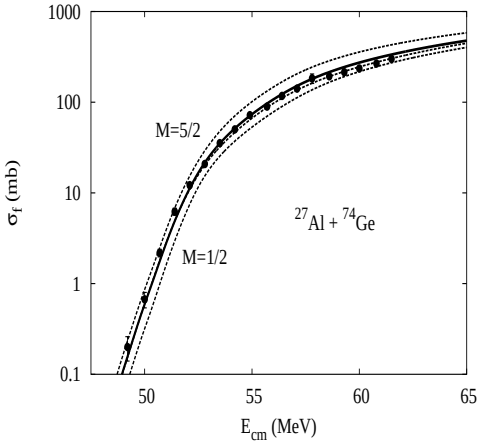

Fig. 1. Fusion cross sections for ^{27}Al+^{74}Ge.

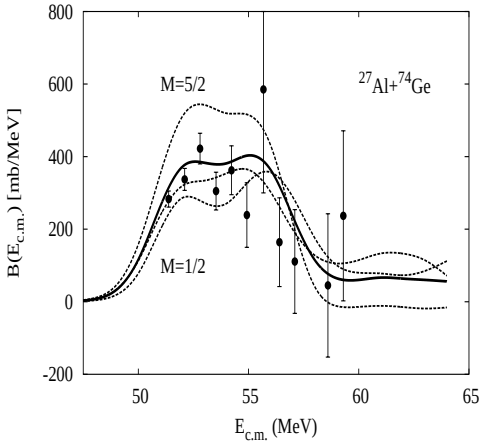

Fig. 2. Barrier distributions for ^{27}Al+^{74}Ge.

§6. Fusion at extreme barrier energies.

The fusion cross sections of several heavy-ion systems have shown an unexpected steep falloff with decreasing energy at energies far below the Coulomb barrier.[5] It has so far not been possible to reproduce this behavior with conventional coupled-channels calculations.[4] Here I illustrate the low energy behavior of calculated fusion cross sections for ^{64}Ni + ^{64}Ni. The calculations are based on the 2^+ state at 1.35 MeV with $\beta_2^C = 0.165$ and $\beta_2^N = 0.185$, and the 3^- state at 3.56 MeV with $\beta_3^N = \beta_3^C = 0.193$. The calculations also include the two-phonon quadrupole excitation and the mutual excitation of the 2^+ and 3^- states. By slightly adjusting the ion-ion potential (2·12) one can obtain an excellent fit to the data[23] as shown in Fig. 3.

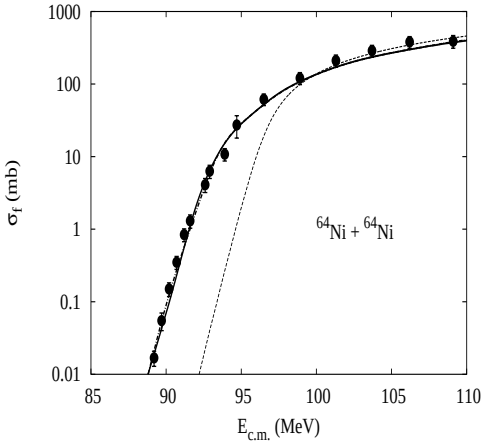

Fig. 3. Fusion cross sections for ^{64}Ni+^{64}Ni. Two coupled-channels calculations (solid and dotted-dashed curves) are compared to data.[23] The dashed curve shows the no-coupling limit.

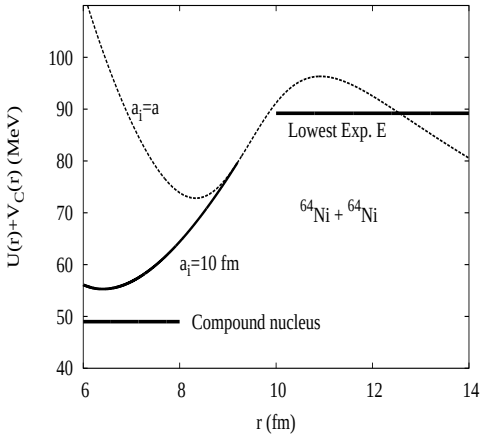

Fig. 4. Coulomb plus nuclear potentials for ^{64}Ni+^{64}Ni. The dashed curve is based on a conventional Woods-Saxon potential. The solid curve has a diffuseness of 10 fm for $r < R_1 + R_2$.

One issue of interest is the sensitivity to the ion-ion potential at short distances. The Coulomb plus nuclear potential is shown in Fig. 4 for a conventional Woods-Saxon parametrization with diffuseness $a = 0.676$ fm (dashed curve). The solid curve shows a modified interaction, which has the diffuseness $a_i = 10$ fm inside the barrier and has been joined smoothly to the conventional interaction at $r = R_1 + R_2$. The modified interaction produces a fusion cross section (the solid curve in Fig. 3) which is almost identical to the conventional result (dotted-dashed curve).

The logarithmic derivatives of the fusion cross sections shown in Fig. 3 are shown in Fig. 5. The result for the one-dimensional barrier penetration rises steeply near the Coulomb barrier (at 96.3 MeV) and levels off at lower energies. The results of the two coupled-channels calculations show a similar behavior, but the steep rise is shifted to lower energies and oscillations occur at even lower energies. The oscillations are a coupled-channels effect caused by the limited number of channels. By choosing the larger diffuseness inside the Coulomb barrier (solid curves in Figs. 3-6) it is possible

to make some improvement in the fit to the logarithmic derivatives extracted from the measurements. A similar result was recently obtained[24] for ^{58}Ni + ^{58}Ni by using a large diffuseness of 1.3 fm, both inside and outside the Coulomb barrier.

The logarithmic derivative extracted from the measurements does not show a clear maximum at low energy but seems to keep increasing with decreasing energy. This feature has been seen for several heavy-ion systems.[4),5)] The logarithmic derivative has even exceeded in some cases the value obtained for a constant S factor, Eq. (4·4). When this occurs the S factors obtained from the measured heavy-ion fusion cross sections will actually exhibit a maximum.[4),19)]

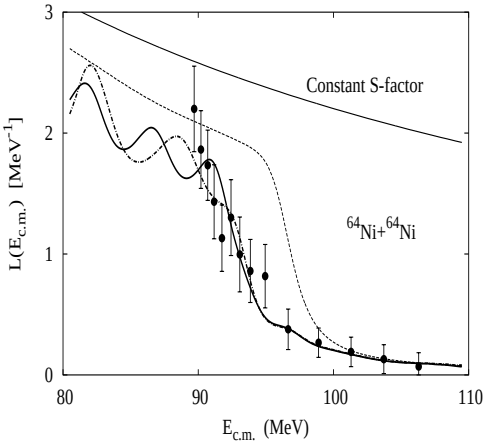

Fig. 5. Logarithmic derivative of the fusion cross sections shown in Fig. 3. The top curve is the result for constant S factor.

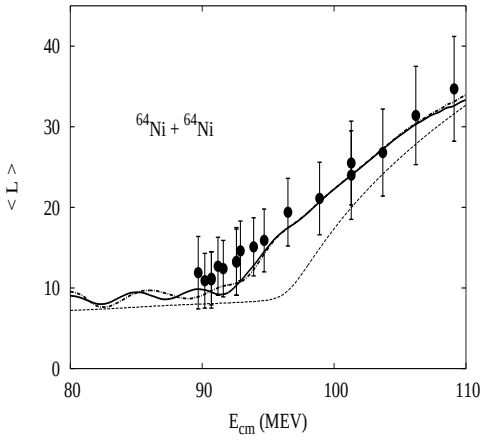

Fig. 6. Average spin of the compound nucleus, extracted from the measured γ-ray multiplicity in ^{64}Ni+^{64}Ni fusion reactions.[23)]

As a final example of a probe of the ^{64}Ni+^{64}Ni fusion reaction I show in Fig. 6 the average spin of the compound nucleus as function of energy. The calculations are the same as those shown in Figs. 3 and 5. The results of the two coupled-channels calculations (solid and dotted-dashed curves) are enhanced compared to the result of the one-dimensional barrier penetration calculation (dashed curve), and they are both in good agreement with the measurements.[23)] It is seen that the calculated average spin is roughly a constant below 90 MeV but there are some oscillations, which are related to those seen in the logarithmic derivatives in Fig. 5.

§7. Summary

I have reviewed the approximations that are commonly made in coupled-channels calculations of heavy-ion fusion reactions. The main reason was to point out theoretical uncertainties in such calculations, and to see what could be the reason why we sometimes have problems in reproducing high precision fusion data.

One problem is that we do not always know the nuclear coupling strengths to low-lying states. To proceed we then assume that they can be obtained from the electromagnetic couplings, but that may not always be a good approximation. It

would therefore be very useful if elastic and inelastic scattering data were available for the same heavy-ion system, so that we could analyze these data within the same coupled-channels calculation that is used to analyze the fusion data.

One of the uncertainties is the determination of the ion-ion potential. I tried to argue that this interaction is rather well established at large radial separations, and that fusion is a very good probe of it in the vicinity of the Coulomb barrier.[3] I also showed that the fusion at energies far below the Coulomb barrier is sensitive to the interaction at even shorter distances.

The coupled-channels calculations we have made so far are not able to reproduce some of the measurements that have been performed at extreme subbarrier energies. There is evidently some kind of hindrance which has not yet been identified. It is possible that the in-going-wave boundary condition, which simulates the fusion process, is too primitive. This is certainly true for heavier systems, where there is competition with deep inelastic reactions and quasi-fission.

Acknowledgements

This work was supported by the U. S. Department of Energy, Nuclear Physics Division, under Contract No. W-31-109-ENG-38.

References

1) A. B. Balantekin and N. Takigawa, Rev. Mod. Phys. **70** (1998), 77.
2) P. R. Christensen and A. Winther, Phys. Lett. B **65** (1976), 19.
3) C. H. Dasso, S. Landowne, and A. Winther, Nucl. Phys. A **407** (1983), 221.
4) C. L. Jiang et al., Phys. Rev. C (in press).
5) C. L. Jiang et al., Phys. Rev. Lett. **89** (2002), 052701.
6) Ricardo A. Broglia and Aage Winther, *Heavy-ion reactions*, Frontiers in Physics Lecture Notes Series Vol. 84 (Addison-Wesley, 1991).
7) K. Hagino, N. Takigawa, and S. Kuyucak, Phys. Rev. Lett. **79** (1997), 2943; Phys. Rev. C **57** (1998), 1349.
8) H. Esbensen and S. Landowne, Phys. Rev. C **35** (1987), 2090.
9) H. Esbensen, J. Q. Wu, and G. F. Bertsch, Nucl. Phys. A **411** (1983), 275.
10) K. Hagino, N. Takigawa, M. Dasgupta, D. J. Hinde, and J. R. Leigh, Phys. Rev. C **55** (1997), 276.
11) G. R. Satchler, Phys. Rep. **199** (1991), 147.
12) B. V. Carlson et al. Phys. Rev. C **41** (1990), 933.
13) K. Hagino, N. Takigawa, M. Dasgupta, D. J. Hinde, and J. R. Leigh, Phys. Rev. Lett. **79** (1997), 2014.
14) J. Gomez-Camacho and R. C. Johnson, J. of Phys. **G12** (1986), L235.
15) O. Tanimura, Phys. Rev. C **35** (1987), 1600.
16) H. Esbensen, S. Landowne, and C. Price Phys. Rev. C **36** (1987), 1216.
17) N. Rowley, G. R. Satchler, and P. H. Stelson, Phys. Lett. B **254** (1991), 25.
18) H. Timmers et al., Nucl. Phys. A **633** (1998), 421.
19) C. L. Jiang, FUSION03, Nov. 12-15, Matsushima, Japan.
20) H. Esbensen, Phys. Rev. C **68** (2003), 034604.
21) E. F. Aguilera et al., Phys. Rev. C **41** (1990), 910.
22) R. Lecomte et al., Phys. Rev. C **22** (1980), 1530.
23) D. Ackermann et al., Nucl. Phys. A **609** (1996), 91.
24) K. Hagino, N. Rowley, and M. Dasgupta, Phys. Rev. Lett. **67** (2003), 054603.